Cost of Increased Bandwidth Efficiency in 5G NR

Toni Levanen*, Kari Pajukoski†, Markku Renfors*, Mikko Valkama*
*Laboratory of Electronics and Communications Engineering, Tampere University of Technology, Finland
†Nokia Bell Labs, Finland
Email: toni.levanen@tut.fi

***Abstract*—In this paper, subband filtered CP-OFDM and windowed CP-OFDM waveforms proposed for 5G new radio (NR) are compared to LTE-like downlink and uplink waveforms under different power amplifier (PA) models. The effects of subband filtering or windowing are evaluated in terms of out-of-band and inband emissions, average error vector magnitude (EVM) and maximum uplink PA output power when increasing the bandwidth efficiency from 90% to 97.2%. The evaluations include recently proposed PA models by 3GPP TSG-RAN WG1 for downlink and uplink. It is shown that the cost of increased bandwidth efficiency in fullband downlink transmission is mainly complexity increase required by the steeper channelization filter. On the other hand, the increased EVM caused by channel filter induced inter-symbol-interference may limit the usability of modulation 256-QAM and above. In uplink with fullband transmission using 64-QAM modulation, the spectral containment is not an issue because the required backoff with highly non-linear PA model limits the Tx power to a very low level independently of the maximum allocation size. In the 1 PRB uplink, increased bandwidth utilization decreases the maximum PA output power while increased backoff improves the inband ACLR.**

***Keywords*—5G, LTE, CP-OFDM, CP-UF-OFDM, f-OFDM, W-OFDM, emission mask, ACLR, power amplifier**

I. Introduction

Orthogonal frequency division multiplexing (OFDM) has been the dominant technique for high throughput wireless communications for the last two decades. OFDM has multiple advantageous features, e.g., robustness against frequency selective fading and narrow-band interference, simple channel equalization and flexible spectrum allocation. Due to these advantages, OFDM is adopted for e.g. in LTE [1] and WiFi [2]. Typically, a cyclic prefix (CP) is added to the OFDM symbol, denoted as CP-OFDM, to remove inter-symbol interference (ISI) between OFDM symbols and to allow the usage of single tap channel estimation and equalization per subcarrier (SC).

Future wireless networks, while providing an improved throughput and user experience for enhanced mobile broadband (eMBB) users, aim also to support mixed numerology or relaxed timing requirements for different services. Different services to be supported together with eMBB inside the same carrier include ultra reliable low latency communications, device-to-device connectivity, and internet-of-things communications. New applications are predicted to use high packet rates with small packets and different physical layer numerology compared to eMBB communications [3].

In this paper, we evaluate and compare the spectral containment of LTE-like signals in a 10 MHz carrier bandwidth under different power amplifier (PA) models. The LTE uplink (UL) and downlink (DL) out-of-band (OOB) emission masks and adjacent channel leakage ratio (ACLR) requirements are defined in [4] and [5], respectively. The LTE-like signals are then compared to recently proposed subband filtered CP-OFDM (F-OFDM) schemes, such as filtered-OFDM (f-OFDM) [6] and universal filtered OFDM with CP (CP-UF-OFDM) [3], [7], and windowed CP-OFDM (W-OFDM), also known as windowed overlap-and-add (WOLA) processing [8], which has been evaluated for LTE already in [9].

In the third generation partnership project (3GPP) technical report [10], it is defined that 5G new radio (NR) should support larger allocations in the same channel bandwidths as used in LTE, for example, 54 physical resource block (PRB) allocation in a 10 MHz carrier bandwidth where 50 PRBs is the current maximum for LTE. This would provide a bandwidth efficiency increase from 90% to 97.2%. We show that LTE solutions with enhanced channel filtering can provide similar OOB emissions and can already support higher bandwidth utilization defined for 5G NR. For inband emissions, on the other hand, the F-OFDM and W-OFDM schemes provide improved inband ACLR between physical resource blocks (PRBs), and therefore improved support for mixing different services having different physical layer (PHY) numerology or relaxed synchronization requirements compared to the eMBB traffic.

In 5G NR, in below 40 GHz communications, a CP-OFDM based enhanced waveform will be used in both DL and UL [10] A DFT-spread-OFDM (DFT-s-OFDM) based waveform, which is also used in LTE UL [1], can be used in coverage limited single stream UL transmission [10] in 5G NR. In this paper, we concentrate on the CP-OFDM based waveforms and their performance especially on high bandwidth utilization cases in DL and UL. For the UL scenarios we include DFT-s-OFDM waveform results for comparison.

This paper is organized as follows. In Section II, the physical layer parameterization and the evaluated enhanced CP-OFDM based waveform candidates are described in more details. In Section III, basic performance evaluation assumptions and PA models used in UL and DL evaluations are first described and then the spectral containment properties of different waveforms are evaluated in terms of OOB emissions and average error vector magnitude (EVM) for UL and DL, and in terms of maximum PA output power and inband ACLR in UL. Finally, in Section IV, conclusions are drawn.

II. Evaluated Waveforms

A. LTE-like CP-OFDM

The baseline parameterization is shown in Table I. The fullband allocation size used in simulations is either 50 PRBs or 54 PRBs, which is one example scenario of increased bandwidth efficiency in 5G NR. The guard period (GP) defined

TABLE I. PHYSICAL LAYER PARAMETERIZATION

Parameter	Value
Common parameters	
Carrier bandwidth	10 MHz
Sampling rate	15.36 MHz
FFT size (N_{FFT})	1024
CP length (N_{CP})	72
Guard period length (N_{GP})	72
Subcarrier spacing (ΔF)	15 kHz
Number of PRBs (N_{PRB})	50 / 54
Number of SCs per PRB	12
Maximum number of active SCs	600 / 648
Number of OFDM symbols per subframe (N_{sym})	14
Detection offset (N_{DO})	0 / 36
DL modulation	256-QAM
UL fullband modulation	64-QAM
UL 1 PRB modulation	QPSK
CP-UF-OFDM parameters	
Filter length (N_f)	37 / 73
Filter type	Dolph-Chebyshev
1 PRB filter side lobe attenuation (SLA)	35 / 40 dB
3 PRB filter side lobe attenuation (SLA)	35 / 60 dB
f-OFDM parameters	
Filter length (N_f)	512
Filter type	Hann-windowed sinc-pulse
Tone offset (54 PRB)	0 / 10
Tone offset (1 PRB)	0 / 4
W-OFDM parameters	
Window slope length (N_{ws})	18 / 72
Window type	Raised cosine

in Table I defines the number of extra samples per subframe partially or fully used by filter transients or time domain windows. If the used channel filter or subband filter causes transients longer than the GP, it is truncated to desired length with a raised cosine window defined, e.g., in [11].

The LTE-like CP-OFDM used in this paper, follows the LTE radio access numerology for 10 MHz carrier bandwidth, except that all CP-OFDM symbols have equal length CP for simplicity. Similar parameterization is proposed also in [10] for 5G NR performance evaluations. The LTE-like CP-OFDM with channel filter is denoted as CP-OFDM from here on. In a modern LTE base station (BS), channel filtering is typically used to achieve the OOB emission masks. The effect of increasing the bandwidth efficiency by allocating 54 PRBs instead of 50 PRBs is mainly seen in the channel filter length. In the presented results, a 219 tap linear-phase FIR channel filter is used to reduce the CP-OFDM OOB emissions to allow the transmitted signal to achieve the emission mask defined in [5] for BS and in [4] for user equipment (UE). If the maximum allocation size is 50 PRBs, a 57 tap channel filter is sufficient, indicating roughly a $4\times$ larger channel filtering complexity for the considered 5G NR scenario. The lengths of channel filters are not fully optimized, but the relative complexity difference for optimized filters can be assumed to be similar. For UL, the same channel filters are used for DFT-s-OFDM signals.

In the case of enhanced F-OFDM waveforms it is typically assumed that the subband filtering is sufficient to achieve the OOB emission masks. In the case of W-OFDM, as will be seen in Section III, the time domain windowing alone is not sufficient to achieve the OOB emission masks and needs to be combined with a channel filter.

B. CP-UF-OFDM

The first introduced F-OFDM scheme is the so called CP-UF-OFDM [3], [7]. The used subband filter is a Dolph-Chebyshev FIR filter of length $N_f = 37$ or $N_f = 73$. The side lobe attenuation (SLA) defined in Table I, is a design parameter used to specify the 3dB-passband of the filter. The UF-OFDM processing is typically associated with zero prefix but can be equally well used with CP [7]. The CP-UF-OFDM design ideology relies on a small number of different, predesigned filters for relatively narrow subbands. In this paper, subband sizes of 1 PRB and 3 PRB are used. The 50 PRB and 1 PRB UL cases are simulated with filter designed for 1 PRB subband and in the 54 PRB transmission case a filter designed for 3 PRB subband is used. For the fullband scenarios, each subband is separately filtered in Tx and Rx with matched subband filters. Tx side pre-equalization is used to remove the Tx filter effect on the amplitude response and on the Rx side corresponding equalization is used to remove the Rx filter inband attenuation.

C. f-OFDM

The second evaluated F-OFDM scheme was introduced in [6], and is entitled as f-OFDM. The used subband filter is based on Hann windowed sinc-function, where the sinc-function is defined based on the allocation bandwidth. The filter length is $N_f = 512$. Because the sinc-pulse width in time depends on the allocation width, the assumed filter causes minimal increase in ISI with wide allocations but may cause significant ISI with narrow allocations, e.g., 1 PRB allocation. The subband wise filtering is performed in both, Tx and Rx, and the Rx filter is matched to the Tx filter. The filter is separately designed for 54 PRB, 50 PRB, and 1 PRB cases. To reduce the inband error vector magnitude (EVM) caused by the very steep filtering, a tone offset (TO) is introduced. TO defines the filter's passband extension as a multiple of SC spacing ΔF. Thus, $TO = 4$ indicates that the passband defined by the sinc-function is $4\Delta F$ Hz wider than the scheduled allocation. For fullband scenarios studied in Section III, the performance is compared with TO=0 and TO=10, and for 1 PRB UL case the performance is compared with TO=0 and TO=4. The increased TO values are used to achieve similar inband EVM as for the reference CP-OFDM waveform. Tx side subband wise pre-equalization and Rx side compensation is used to alleviate the EVM increase caused by inband attenuation with f-OFDM.

D. W-OFDM

The evaluated time domain windowed CP-OFDM (W-OFDM) is a widely known computationally efficient method to reduce the side lobe power of CP-OFDM signals, and is also known as windowed overlap-and-add (WOLA) [9], [8]. It has been introduced for 5G NR as a low complexity candidate method to allow improved inband ACLR to support mixed numerology and asynchronous traffic. The W-OFDM scheme used in this article uses only one window, for simplicity, and no multi-window schemes are studied. Example of a multi-window scheme can be found from [11].

In W-OFDM, the CP-OFDM symbol is extended by N_{ext} samples, and the number of extended samples equals to the window slope length $N_{\text{ws}} = N_{ext}$. Window slope length defines the rising and falling edge of the window in samples. The total window length is $N_{win,Tx} = N_{FFT} + N_{CP} + N_{\text{ws}}$. After windowing, an overlap-and-add processing is used to partially overlap adjacent windowed CP-OFDM symbols to reduce the overhead caused by windowing and to retain the

original symbol timing. The used window is a raised cosine window [11].

In the Rx side, the windowing and overlap-and-add processing is performed within the CP-OFDM symbol. The used window length is $N_{win,Rx} = N_{FFT} + N_{\text{ws}}$. In other words, in the Rx processing the received CP-OFDM symbol is not extended before WOLA processing, as indicated also in [8].

In Section III, the W-OFDM performance is studied with two different window slope lengths, namely $N_{\text{ws}} = 18$ and $N_{\text{ws}} = 72$. The shorter window length is sufficient to allow operation in the 50 PRB case, but not in the 54 PRB case. For this reason, we provide an example of combined W-OFDM and channel filtering processing in Section III-B. The channel filter used with W-OFDM in 54 PRB case is of length 151 samples, which indicates roughly a 31% reduction in the channel filter length when combined with W-OFDM processing.

III. Cost of Increased Bandwidth Efficiency

In this section, the considered 5G NR waveform candidates are compared against the LTE-like CP-OFDM signal under different power amplifier models, and the effect of increasing bandwidth efficiency from 90% to 97.2% is evaluated through numerous examples. If the same maximum modulation and coding scheme can be supported with increased bandwidth efficiency, it is directly translated into increased spectral efficiency. First, fullband allocation results are evaluated for DL and UL. These can be considered as high throughput scenarios. As discussed in Section I, 5G NR should support larger allocations in the LTE channel bandwidths. In fullband results, 54 PRB and 50 PRB allocations in 10 MHz LTE channel are compared. In the second set of results, UL transmission with 1 PRB allocation is studied and OOB and inband ACLR are evaluated and compared with maximum number of 50 PRBs or 54 PRBs. The 1 PRB case is considered as a high coverage scenario, where the maximum PA output power instead of throughput is the most interesting performance indicator.

A. Performance Evaluation Assumptions

The general physical layer parameterization was provided in Table I. Next we focus on specific aspects related to the results presented later in this section.

The PA models used in this paper have been introduced for performance evaluations below 6 GHz communications in 3GPP TSG-RAN WG1. The DL PA model is introduced in [12] and UL PA model in [13]. These models are used because they are openly available and commonly agreed to provide a good starting point for spectral containment evaluations regarding 5G NR. The DL PA model is a modified Rapp model. The PA model mimics a BS PA including some crest factor reduction and digital predistortion schemes to linearize the BS PA to achieve the LTE emission mask with 10 MHz fully populated 64-QAM signal. The PA is parameterized to provide 46 dBm output power for 10 MHz fully populated LTE signal with 50 PRBs and 64-QAM modulation an OOB ACLR of 45 dB, and meeting the respective LTE DL OOB emission masks. The UL PA model is a polynomial model of order nine obtained by fitting a polynomial to measurements from a commercial UE PA [13]. The polynomial model should be used only with PA input levels between -30 dBm and 9 dBm. The 1 dB input referred compression point is at $P_{1dB} = 3.4$ dBm and the model is parametrized to provide 26 dBm PA output power, corresponding to the 1 dB maximum power reduction [4], with 20 MHz QPSK modulated fully populated LTE uplink signal (100 PRB allocation), while meeting the minimum UL ACLR requirement of 30 dB for E-UTRA.

The transmitted signal power spectral density (PSD) is evaluated per subframe basis, where each subframe carries 14 data symbols. The PSD results are obtained by averaging 100 independent realizations of subframes. The PSD is obtained by taking an $N_{FFT,PSD} = 4[N_{sym}(N_{\text{FFT}} + N_{\text{CP}}) + N_{\text{GP}}]$ point FFT of the subframe after the PA model. All the results are shown by using a 30 kHz measurement bandwidth over the frequency range and the OOB emission limits defined in [4] or [5] corresponding to this measurement bandwidth. No control signal or reference symbols are assumed for simplicity. The specific design of control and reference symbols for 5G NR is currently an open topic, so their effect on the waveform PSD is left for future research. To each subframe, a guard period (GP) is added to incorporate possibly truncated filter transients or time domain window transients. Truncation of filter transients is done with a raised cosine window.

At the receiver side, a detection offset is introduced for the EVM evaluations. In this paper, detection offset of $N_{\text{DO}} = 36$ samples is used in all evaluations, indicating that the Rx FFT window starts from the middle of the CP. In fullband DL transmission case (see Table II), the effect of detection offset is evaluated with values $N_{\text{DO}} = 0$ and $N_{\text{DO}} = 36$. If $N_{\text{DO}} = 0$, then the whole CP is discarded and the Rx FFT window is located at the end of the CP-OFDM symbol. We chose to show these two extremes of detection offset, because with $N_{\text{DO}} = 0$ the filtering or windowing induced ISI is maximized and with $N_{\text{DO}} = 36$ the ISI is minimized. The inband EVM is evaluated by inserting the PA output into a waveform detector without an equalizer. Extra samples are removed according to detection offset introduced earlier, and the remaining part is inserted to the Rx FFT. From the FFT output, the allocated subcarriers (SCs) are collected and they are compared to the transmitted symbols to evaluate the average inband EVM. It should be emphasized that the used method does not exactly follow the specifications given in [4] or [5].

In LTE [4], the UL inband spectrum emission mask is based on the power spectral densities after the Rx FFT processing. Using a similar approach in 5G with mixed numerology scenarios could lead to extra evaluation and verification complexity. This is due to the fact that all different numerology combinations need to be evaluated through both the victim's and the aggressor's Rx FFT and numerology dependent inband emission masks are required. To simplify the comparison, here it is proposed that similarly to OOB emission evaluations, the inband emission evaluations would be based on subframe wise PSDs. This way there is no need to specify different inband emission masks for different numerologies or services, as the same mask would apply to all. The inband emission and ACLR results presented for 1 PRB case in Section III-D are based on the proposed approach. For the given 1 PRB results, we have verified that they all fulfill the LTE UL inband emission mask. In practice, independently of the method used to define inband emissions, numerology wise EVM evaluation is required for verifying the performance of two neighboring

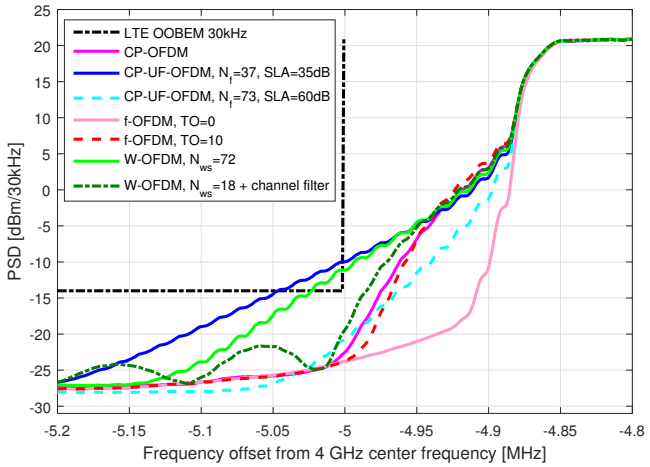

Fig. 1. PSDs for evaluated waveforms and LTE mask in DL with 3GPP Rapp PA model using 54 PRBs and 256-QAM modulation

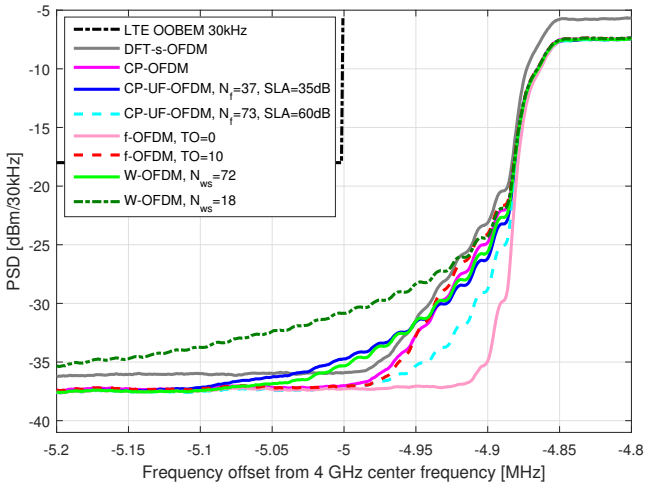

Fig. 2. PSDs for evaluated waveforms and LTE UL emission mask with 3GPP polynomial PA model using 54 PRBs and 64-QAM modulation

TABLE II. AVERAGE EVMS FOR 3GPP DL RAPP PA MODEL

Waveform	Average EVM [%]			
	Detection offset 0		Detection offset 36	
	50 PRB	54 PRB	50 PRB	54PRB
CP-OFDM	0.8	1.0	0.5	0.6
CP-UF-OFDM, $N_f = 37$	4.1	5.0	0.5	0.5
CP-UF-OFDM, $N_f = 73$	6	9.7	0.7	0.6
f-OFDM, TO=0	2.0	1.9	1.1	1.1
f-OFDM, TO=10	1.1	1.0	0.5	0.5
W-OFDM, $N_{ws} = 18$	0.5			
W-OFDM, $N_{ws} = 72$	0.7			
W-OFDM, $N_{ws} = 18$+ch. filt.	0.8			

TABLE III. MAXIMUM PA OUTPUT POWERS FOR 3GPP UL POLYNOMIAL PA MODEL WITH AVERAGE EVM LIMIT 5%

Waveform	IBO [dB]	PA output power [dBm] 50 PRB and 54 PRB
DFT-s-OFDM	10.9	19.4
CP-OFDM	12.5	17.8
CP-UF-OFDM, $N_f = 37$	12.6	17.6
CP-UF-OFDM, $N_f = 73$	12.6	17.6
f-OFDM, TO=0	12.6	17.6
f-OFDM, TO=10	12.5	17.8
W-OFDM, $N_{ws} = 18$	12.6	17.6
W-OFDM, $N_{ws} = 72$	12.6	17.6

received signals using different numerologies (or different synchronization requirements).

B. Fullband DL Results

The LTE OOB emissiom mask (OOBEM) for 30 kHz measurement bandwidth and PSDs of waveforms described in Section II are shown in Fig. 1 for a 54 PRB DL transmission. In DL evaluations with the Rapp PA model the transmit power is fixed to 46 dBm. In Fig. 1, an example of the W-OFDM with channel filtering is given. In this case, W-OFDM with $N_{\text{ws}} = 18$ would clearly not fulfill the DL OOBEM, but when combined with reduced complexity channel filter could eventually achieve the emission mask. Also, W-OFDM with $N_{\text{ws}} = 72$ or CP-UF-OFDM with $N_f = 37$ do not achieve the DL OOBEM.

Inband EVMs achieved by different waveforms are in interest of this scheme and are shown in Table II. Because the DL PA model incorporates crest factor reduction and PA linearization, the measured average EVMs do not model actual PA induced EVMs, but rather the additional error on top of algorithms used to linearize the DL PA which is eventually of primary interest anyway as meeting the DL ACLR requirements is not feasible without linearization. In Table II, the average EVM with or without detection offset with 50 or 54 PRB allocation is given. First observation is that the detection offset used in evaluation has a clear impact on the measured EVM, expecially with CP-UF-OFDM due to the time domain response of the Dolph-Chebyshev filter. Among waveforms achieving the DL OOBEM, f-OFDM with $TO = 10$ and CP-OFDM provide the best average EVM. For W-OFDM waveform, only one EVM value is given because the used allocation size or detection offset parameter do not affect the W-OFDM receiver operation. Because there is no equalizer included in the EVM evaluations, the presented EVM values can be considered as upper limits for the PA induced distortion. The results also indicate that the average EVM of a fullband DL transmission is relatively insensitive to increased bandwidth efficiency, as expected. For example, with CP-OFDM the effect is visible in a few SCs close to the channel edge which have a clearly lower EVM in 54 PRB case than in 50 PRB case, but this effect is hidden when averaging over large number of SCs. This also indicates that to allow efficient multiplexing of relatively narrow allocations of high modulation and coding scheme (MCS) DL signals for different UEs, the edge PRB EVM should be separately evaluated to ensure that highest MCS is usable in all PRBs with all different allocation sizes.

In general, all evaluated waveforms have rather similar DL fullband performance in terms of transmitted signal spectrum. The CP-OFDM signal (with channel filter) is well capable to achieve the LTE OOB emission mask and new waveform candidates do not bring any clear improvement with respect to OOB emissions.

C. Fullband UL Results

In UL, the transmit power is not fixed to any specific power level like in DL modeling. Hence, the transmitted power can be increased as long as EVM and OOB emission and

ACLR requirements are satisfied. Tx power is controlled in evaluations by adjusting the input backoff (IBO) value of the PA. PSDs of the evaluated waveforms together with LTE UL OOBEM in 54 PRB case are shown in Fig. 2 assuming 64-QAM modulation. For UL results, we include also the DFT-s-OFDM waveform as a reference.

For each waveform, the transmit power is maximized by reducing IBO value of the power amplifier as much as possible. A brute force search over IBO values with 0.1 dB accuracy was performed to get the Tx signal EMV as close as possible to the 5% limit to examine the maximum PA output power for each waveform. The EVM requirement was obtained from [5], where 8% requirement for 64-QAM is defined. Here it was assumed that PA may contribute 5% of the total EVM, and rest of the distortion is caused by other sources, such as phase noise, I/Q-imbalance, etc. For all waveforms, EVM requirement of 5% is the limiting factor as ACLR and LTE UL OOBEM are fulfilled with clear (see Fig. 2) margin. Table III shows maximized PA output powers and corresponding IBO values. There is no difference in the maximum PA output power in the fullband UL case, because the average EVM is dominated by the non-linear distortion induced by the PA model.

When IBO is minimized for each individual waveform, differences in spectral containment between waveforms are not significant as shown in Table III. All evaluated multicarrier waveforms achieve the EVM target roughly with the same IBO. DFT-s-OFDM has approximately 1.7 dB gain against multicarrier waveforms. The very low PA output powers are mainly due to the missing equalizer in the EVM analysis and selected evaluation scheme. Also the highly non-linear UE PA model affects the results, which implies that in the UL the differences between waveform signal processing techniques to achieve better subband-wise spectral containment are reduced, especially in the case of fullband transmission. It is clear that some methods to reduce the PAPR of the fullband UL transmission are required in 5G NR. On the other hand, as the 5G NR UL will support even larger modulations, e.g. 256-QAM currently studied for LTE UL, one can expect that more linear UL PAs are required for 5G high category devices which will alleviate the power backoff problem. As in the case of fullband DL, CP-OFDM can cope with increased bandwidth efficiency as well as the new waveform candidates. In general, the increased bandwidth efficiency has a relatively small impact on the fullband UL performance with the used polynomial PA model.

D. 1 PRB UL Results

The 1 PRB UL case is considered to be very important from two different perspectives. It can be considered as the minimum allocation for a eMBB UE in a coverage limited case, or it can be considered as a low rate device from different service category transmitting inside the eMBB carrier. In both cases, the most interesting metric is the maximum PA output power. For this reason, in the 1 PRB case the used modulation is reduced to QPSK. This is intuitive, because 1 PRB transmission is maximizing the coverage by maximizing the Rx power spectral density in the BS side rather than throughput. For the maximum PA output power we assume that 27 dBm is the allowed maximum. With 4 dB of losses

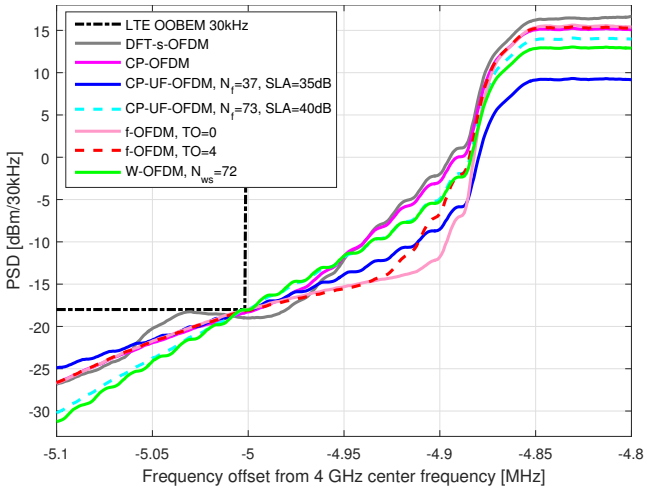

Fig. 3. PSDs for evaluated waveforms with LTE UL emission mask in the case of 1 PRB UL transmission with maximum allocation of 54 PRBs

TABLE IV. USED IBO AND ACHIEVED MAXIMUM PA OUTPUT POWER AND EVM FOR UL POLYNOMIAL PA MODEL WITH 1 PRB TRANSMISSION

Waveform	Parameters		
	IBO [dB]	PA output power [dBm]	EVM [%]
Maximum allocation size 50 PRBs			
DFT-s-OFDM	3.1	27.0	8.5
CP-OFDM	4.6	25.4	11.8
CP-UF-OFDM, $N_f = 37$	4.6	25.4	11.8
CP-UF-OFDM, $N_f = 73$	4.6	25.4	11.9
f-OFDM, TO=0	4.9	25.2	11.9
f-OFDM, TO=4	4.7	25.3	11.9
W-OFDM, $N_{ws} = 18$	4.6	25.4	11.8
W-OFDM, $N_{ws} = 72$	4.6	25.4	12.0
Maximum allocation size 54 PRBs			
DFT-s-OFDM	6.4	24.3	8.0
CP-OFDM	7.5	23.0	7.2
CP-UF-OFDM, $N_f = 37$	13.1	17.1	4.1
CP-UF-OFDM, $N_f = 73$	8.7	21.8	7.3
f-OFDM, TO=0	7.3	23.2	8.8
f-OFDM, TO=4	7.4	23.1	7.3
W-OFDM, $N_{ws} = 72$	9.7	20.8	7.1

after the PA this leads to 23 dBm of radiated power which is typically the maximum in LTE bands [4].

Another important metric is the inband ACLR. High inband ACLR improves the support for mixed numerology transmission schemes inside a 5G NR carrier. Power leakage to other resource blocks causes inter-subband-interference forcing the use of larger guard bands (GBs) between different services, which in turn degrades the spectrum efficiency. Furthermore, if the Tx signal is not well frequency localized, the interference can not be sufficiently removed by Rx filtering as the interference is already inside the desired Rx subband.

In these evaluations, the allocated PRB is located as close to the channel edge as possible on the left hand side of the target channel (PRB index 0 in LTE). The PSDs of 1 PRB UL signals in maximum allocation of 54 PRB case for different waveforms together with LTE OOBEM are illustrated in Fig. 3, such that maximum PA output power is obtained while meeting all the emission requirements.

Here it is assumed that PA can contribute 12% EVM and rest is assumed to be generated by other sources. The allowed average EVM level for QPSK specified in [4] is 17.5%. When IBO value is decreased in order to increase Tx power, the

LTE mask becomes a limiting factor in the 54 PRB maximum allocation case. EVM values of each waveform are below 12% with large margin. Maximum achievable Tx powers, without exceeding the LTE UL OOBEM, are listed together with corresponding IBO values in Table IV for maximum allocation sizes of 50 PRBs and 54 PRBs. In the case of 50 PRB maximum allocation, DFT-s-OFDM achieves the target PA output power of 27 dBm and multicarrier waveforms lose approximately 1.6 dB. Overall, the differences in the PA output power or average EVM are rather small among multicarrier waveforms.

When the maximum allocation is increased to 54 PRBs, even DFT-s-OFDM is not able to achieve the 27 dBm PA output power, and provides only 24.3 dBm of PA output power. From Table IV, it is clearly visible that the differences between the new waveform candidates largely increase in the 54 PRB case, and they lose from 1.1 dB to 7.2 dB to DFT-s-OFDM in terms of PA output power. This is one of the key findings of this article. Time domain windowing does not lower the sidelobes as efficiently as filtering which leads to a relatively lower maximum transmit power for the W-OFDM waveform in order to satisfy the LTE emission mask. CP-UF-OFDM with $N_f = 37$ also suffers from the poor spectral containment. Steep filtering of f-OFDM with TO=0 waveform causes distortion for a few edge SCs increasing the average inband EVM. This applies especially in the 1 PRB case, where the total number of active SCs is relatively low compared to highly distorted edge SCs. Introducing a passband extension of TO=4, edge SCs are not as close to the subband filter's transition bands and therefore are less distorted. Because of the used detection offset $N_{\text{DO}} = 36$, the EVM results of the highly selective subband filtered candidates are optimistic, as indicated in Table II. For all waveforms the Tx power is limited by the UL OOBEM and the average EVMs are well below the 12% target value.

The increased total allocation size of 54 PRBs clearly limits the maximum UL Tx power in the 1 PRB transmission case, because the LTE OOB emission mask becomes the limiting factor. In simulations with maximum of 50 PRB allocation, the excess bandwidth allows to use clearly larger Tx powers. So increasing the overall system bandwidth utilization efficiency may limit the UL coverage, especially for the channel edge PRBs. This problem can be eased by scheduling cell edge UEs to the center of the channel, so that the OOB emission requirements are not limiting the Tx power. In this case the scheduler needs to have the capability to evaluate the effect of power leakage from the cell edge transmission not to compromise the required received signal-to-interference-and-noise (SINR) of the neighboring UL signals. In addition, the increased bandwidth utilization may compromise the maximum transmission power required by ultra reliable low latency communications and should therefore be considered with caution is specific use cases.

The inband ACLR is evaluated as the ratio of the average power inside the 1 PRB allocation versus the leakage power inside a 1 PRB band with a given offset defined by the GB. The UL PA model is included in these evaluations. ACLR at four neighboring PRBs are listed in Table V modeling a scheme where the GB size is given in multiple of PRBs, which can be implemented easily with a proper scheduling.

TABLE V. INBAND ACLR AT THE 1ST, 2ND, 3RD, AND 4TH NEIGHBORING PRB WITH 1 PRB UL TRANSMISSION

Waveform	Inband ACLR [dB]			
	1st PRB	2nd PRB	3rd PRB	4th PRB
Maximum allocation size 50 PRBs				
DFT-s-OFDM	17.3	28.5	32.7	35.4
CP-OFDM	16.9	28.6	32.7	35.3
CP-UF-OFDM, $N_f = 37$	17.3	33.1	45.1	55.3
CP-UF-OFDM, $N_f = 73$	18.1	38.2	52.4	63.4
f-OFDM, TO=0	21.3	39.7	55.6	67.2
f-OFDM, TO=4	19.1	39.1	54.3	67.0
W-OFDM, $N_{ws} = 18$	17.0	29.9	36.1	41.4
W-OFDM, $N_{ws} = 72$	17.6	37.6	51.1	61.6
Maximum allocation size 54 PRBs				
DFT-s-OFDM	18.1	29.3	33.4	36.0
CP-OFDM	18.1	29.2	33.2	35.9
CP-UF-OFDM, $N_f = 37$	18.7	35.5	49.8	65.6
CP-UF-OFDM, $N_f = 73$	19.7	44.9	60.5	68.9
f-OFDM, TO=0	23.8	43.5	61.2	69.0
f-OFDM, TO=4	21.0	43.3	60.9	69.3
W-OFDM, $N_{ws} = 72$	19.1	44.4	57.9	67.4

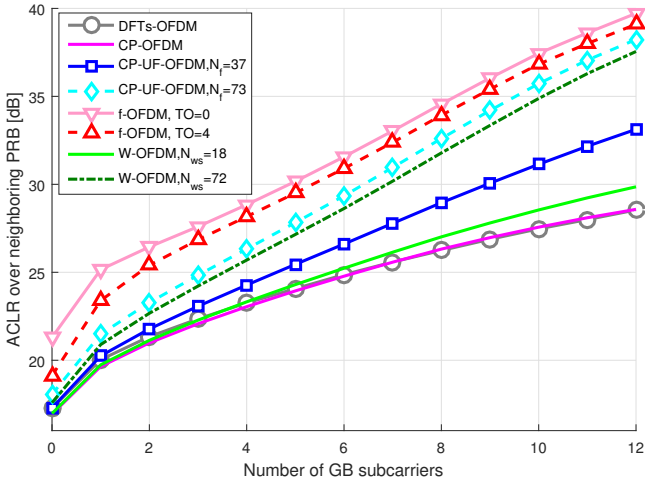

Fig. 4. Inband ACLR as a function of a subcarrier wise GB for the 1 PRB UL transmission with maximum 50 PRB allocation.

In the Table V, the PRB wise inband ACLR for different waveforms for the two maximum allocations sizes is given. The inband ACLR performance of CP-OFDM and DFT-s-OFDM signals are clearly worse after the first neighboring PRB compared to other waveforms due to the channel filtering. At the second PRB, the new waveform candidates provide up to 11.2 dB improvement in the 50 PRB case and up to 15.6 dB improvement in the 54 PRB case in the inband ACLR. For the third and fourth PRB the ACLR values are improved further, but these are not seen that interesting because the required GB would already be causing a significant overhead and the inband ACLR achieved with 1 PRB GB is sufficient for 256-QAM (EVM requirement 3.5% corresponds to 29.1 dB). Among all measured ACLRs, the best ACLR performance is achieved by using f-OFDM with TO=0, as expected, with the cost of 1.5% larger average EVM than with TO=4 in the 54 PRB case. For W-OFDM with $N_{\text{ws}} = 18$, ACLR improvements are modest against the CP-OFDM in the first and second PRB, whereas the channel filter complexity can be reduced approximately 31% compared to CP-OFDM as pointed out in Section II-D. Also, W-OFDM with short window slope length allows to support 256-QAM with 1 PRB GB, and therefore could be considered as an implementation option when combined with channel filtering, at least for 5G NR phase 1.

Another possibility is to allow GB size to be multiple of SCs instead of PRBs. This requires additional signaling between the BS and UE to indicate how many SCs are used as a GB. Improvement of inband ACLR, when increasing the GB by multiples of SCs is illustrated in Fig. 4 for the 50 PRB case. In Fig. 4, GB=0 equals to *ACLR of 1st RB* and GB=12 equals to *ACLR of 2nd RB* case in Table V. With small GB values the differences between waveforms are smaller and increased GB improves the performance of windowed and subband filtered waveforms compared to CP-OFDM or DFT-s-OFDM.

IV. Conclusion

In this paper, subband filtered CP-OFDM and windowed CP-OFDM waveform candidates proposed for 5G NR were compared to LTE-like CP-OFDM and DFT-s-OFDM signals assuming an increased bandwidth efficiency. The evaluated bandwidth efficiencies of 90% and 97.2% assume that 50 or 54 PRBs, respectively, can be scheduled in a 10 MHz carrier. Evaluations included fullband UL and DL schemes as well as 1 PRB channel edge UL transmission scheme reflecting the UL coverage assessment. Recently proposed and openly available DL and UL PA models agreed on 3GPP TSG-RAN WG1 were used in the evaluations.

It was shown that LTE-like processing can support 54 PRB transmissions in UL and DL in terms of OOB emissions. In addition, a full 54 PRB allocation can be supported in all tested cases with similar Tx powers as with 50 PRB allocation. With windowed CP-OFDM, in the fullband DL case, the LTE DL OOB emission mask is slightly exceeded. It was shown that a possible implementation setup for the phase 1 rollout of 5G NR is to use a windowed CP-OFDM with short time domain window and relatively short channel filter to suppress the OOB leakage. This combination allows to support 54 PRB allocations with reduced complexity. In general, the differences in the fullband cases between all evaluated waveforms are small, excluding the larger PA output power facilitated by DFT-s-OFDM in UL. These results indicate that solutions following LTE-like channel filtering can be designed to support higher bandwidth utilization in 5G new radio and to achieve the related OOB emission requirements. The cost, especially in DL, is the increased complexity of the channelization filter and possibly increased EVM caused by longer channel filter induced ISI between CP-OFDM symbols.

In 1 PRB UL transmission, the maximum transmission power and inband ACLR are important metrics for the 5G NR physical layer performance in terms of cell coverage and mixing different services in UL inside one carrier. Subband filtered and windowed CP-OFDM provide clearly lower inband ACLR compared to the reference CP-OFDM or DFT-s-OFDM waveforms and can operate with significantly narrower GBs when considering inband mixed numerology or asynchronous transmissions. In the 1 PRB UL case, only DFT-s-OFDM achieved the target PA output power of +27 dBm in 50 PRB case whereas it lost almost 3 dB of this maximum power in the 54 PRB case. In the 54 PRB case, there are clear differences between the 5G NR waveform candidates as they provide from 1.1 dB up to 7.2 dB smaller maximum PA output power than DFT-s-OFDM. These results indicate that increasing the bandwidth efficiency may limit the coverage of the edge most PRBs and their coverage, e.g., in ultra reliable communication cases. This can be partially solved by scheduling the cell edge UEs to the middle of the channel, where they are not limited by the out-of-band emissions, as long as the inband emission limits are fulfilled. On the other hand, as the PA output powers were reduced, the increased backoff reduced the UL PA induced spreading thus improving the inband ACLR.

Thus, increasing bandwidth utilization does not come for free and requires improved, low complexity signal processing for spectral containment and more linear PAs in the UL not to limit the coverage of the edge most PRBs. Still, the standardization should allow bandwidth utilization close to 100% to allow room for technological development to allow 5G NR to fully achieve its capacity by future evolution.

Acknowledgment

This work was partially supported by the Finnish Funding Agency for Technology and Innovation (Tekes) and Nokia Bell Labs, under the projects "Wireless for Verticals (WIVE)", "Phoenix+" and "5G Radio Systems Research".

References

[1] "3GPP TS 36.300 v. 13.3.0, "Evolved Universal Terrestrial Radio Access (E-UTRA) and Evolved Universal Terrestrial Radio Access Network (E-UTRAN); Overall Description; Stage 2", Tech. Spec. Group Radio Access Network, Rel. 13," March 2016.

[2] "IEEE Standard for Information technology–Telecommunications and information exchange between systems Local and metropolitan area networks–Specific requirements Part 11: Wireless LAN Medium Access Control (MAC) and Physical Layer (PHY) Specifications," *IEEE Std 802.11-2012 (Revision of IEEE Std 802.11-2007)*, pp. 1–2793, March 2012.

[3] G. Wunder, P. Jung, M. Kasparick, T. Wild, F. Schaich, Yejian Chen, S. Brink, I Gaspar, N. Michailow, A Festag, L. Mendes, N. Cassiau, D. Ktenas, M. Dryjanski, S. Pietrzyk, B. Eged, P. Vago, and F. Wiedmann, "5GNOW: non-orthogonal, asynchronous waveforms for future mobile applications," *Communications Magazine, IEEE*, vol. 52, no. 2, pp. 97–105, February 2014.

[4] "3GPP TS 36.101 v. 13.3.0, "Evolved Universal Terrestrial Radio Access (E-UTRA); User Equipment (UE) Radio Transmission and Reception," Tech. Spec. Group Radio Access Network, Rel. 13," March 2016.

[5] "3GPP TS 36.104 V13.3.0, "Evolved Universal Terrestrial Radio Access (E-UTRA); Base Station (BS) Radio Transmission and Reception," Tech. Spec. Group Radio Access Network, Rel. 13," March 2016.

[6] X. Zhang, M. Jia, L. Chen, J. Ma, and J. Qiu, "Filtered-OFDM - Enabler for Flexible Waveform in the 5th Generation Cellular Networks," in *2015 IEEE Global Communications Conference (GLOBECOM)*, Dec 2015, pp. 1–6.

[7] R. Ahmed, T. Wild, and F. Schaich, "Coexistence of UF-OFDM and CP-OFDM," in *2016 IEEE 83rd Vehicular Technology Conference (VTC Spring)*, May 2016, pp. 1–5.

[8] Qualcomm, "5G Waveform & Multiple Access Techniques," 2015.

[9] "3GPP TR 25.892 V6.0.0, "Feasibility Study for Orthogonal Frequency Division Multiplexing (OFDM) for UTRAN enhancement," Tech. Spec. Group Radio Access Network, Rel. 6," June 2004.

[10] "3GPP TR 38.802 v. 2.0.0, "Study on New Radio (NR) Access Technology; Physical Layer Aspects," Tech. Spec. Group Radio Access Network, Rel. 14," March 2017.

[11] A. E. Loulou, S. Afrasiabi Gorgani, and M. Renfors, "Enhanced ofdm techniques for fragmented spectrum use," in *Future Network and Mobile Summit (FutureNetworkSummit), 2013*, July 2013, pp. 1–10.

[12] Alcatel-Lucent Shanghai Bell Nokia, "R1-167297, [85-18] PA assumptions for NR," 2016.

[13] T. Saynajakangas, "R1-166004, Response LS on realistic power amplifier model for NR waveform evaluation," 2016.